INTERNATIONAL JOURNAL OF PHARMACEUTICAL EXCIPIENTS

Preparation and evaluation of minoxidil nanoemulgel topical formulations.

Alaa Al-Taie[a*], Myasar M. Al-Kotaji[b*], Hani M. Al-Mukhtar[a]

[a]College of Pharmacy, University of Mosul, Mosul, Iraq.
[b]College of Pharmacy, Ninevah University, Mosul, Iraq.

Received: June 24, 2024*; Accepted:* November 5, 2024

Original Article

ABSTRACT

The delivery of minoxidil using conventional topical solutions suffers from short contact time with the scalp, poor drug penetration, and high dose requirements. This work aimed to prepare an o/w nanoemulsion-based gel of minoxidil with the goal to prolong contact time with the scalp and possibly enhancing skin permeation. Clove oil was selected as an oil phase, Tween® 80 was selected as surfactant and ethanol was selected as a co-surfactant, and distilled water was used as an aqueous phase while propylene glycol (PG) was used as the co-solvent. Eight formulations of minoxidil loaded nanoemulsion were prepared and subjected to different investigational studies such as measurement of pH, electrical conductivity, percent of light transmittance, entrapment efficiency, droplet size, polydispersity and zeta potential. Moreover, three different minoxidil-loaded nanoemulgel formulations were prepared by using a selected formula of nanoemulsion with three different concentrations of Carbopol® 934. The prepared nanoemulgel formulations were further subjected to characterization studies such as, measurement of pH, spreadability, viscosity, in-vitro drug release and permeation studies to determine the best minoxidil-loaded nanoemulgel formula. The results of the characterization studies showed that the minoxidil loaded nanoemulsion NE-A2 formula with Smix ratio (2:1), 5% oil concentration, and 40% Smix concentration was the optimized formula (hydrodynamic diameter of 14.62 nm ±1.36, PDI of 0.22 ±0.021, zeta potential of - 4.7 ±0.6 and entrapment efficiency of 91.2 ±0.31). The characterization results for the optimized minoxidil-loaded nanoemulgel formula NEG-A2y demonstrated that the formula has an acceptable pH value 6 ± 0.08 with optimum spreadability (21.6 ±0.73 g.cm/s), and optimum viscosity (492 ±87.81 mPa.s) for a nanoemulgel applied topically. The cumulative release profile of the optimized minoxidil-loaded nanoemulgel formulation, NEG-A2y, was slower than that of an alcoholic standard solution and the marketed solution. In addition, the permeation study results showed that the optimized nanoemulgel formula NEG-A2y exhibited a better permeation profile than the marketed solution. The current study succeeded in producing a minoxidil nanoemulgel with enhanced delivery, prolonged contact time, enhanced permeation, and consequent enhanced pharmaco-dynamic effects of minoxidil.

*Corresponding address: Alaa Al-Taie, College of Pharmacy, University of Mosul, Mosul, Iraq, Tel: +9647719743059, E-Mail: alaa_altaie@uomosul.edu.iq

KEY WORDS: Minoxidil, nanoemulgel, nanoemulsion-based gel, nanoemulsion, alopecia

INTRODUCTION

Alopecia is one of the most common dermatological disorders in many communities. It causes many economic and psychological problems. Minoxidil (MXD) was first developed as an oral agent for the treatment of hypertension. Topical solutions of MXD with two dose strengths (2% and 5%) were approved by the FDA in 1991. Later, MXD was used as an off-label drug to treat alopecia areata (AA) as well as to improve body hair growth in other areas including the eyebrows and beard (1).

Because of its poor aqueous solubility, conventional marketed topical preparations of MXD, such as spray, solution, foam, and shampoo products containing MXD in concentrations ranging from 1 to 5%, are currently formulated with organic solvents and co-solvents such as ethanol and PG. Long-term use of such organic solutions can result in the formation of MXD crystals due to ethanol evaporation, which may cause many undesired side effects which limit their usefulness in addition to the requirement for employing relatively high doses to overcomes losses and achieve efficacy (2, 3).

Another major drawback to such preparations is the short contact time with the scalp. Accordingly, huge efforts have been made to increase the contact time, enhance skin penetration to the scalp hair follicles and attain controlled release of the drug for a prolonged period of time with consequent reduction in the frequency of application and to improve patient compliance (4). Thus, it was desirable to develop an alternative topical drug delivery system that can overcome the limitations of conventional formulations such as incorporation of MXD in a nanoemulsion system for topical treatment of alopecia (5).

Nanoemulsions (NEs) are transparent colloidal dispersion systems consisting of a mixture of two immiscible liquids; either oil-in-water (o/w) or water-in-oil (w/o), with the mean droplet size less than 500 nm. The small droplet size of NEs results in clear or translucent solutions, that differ from the milky or white conventional emulsions, and affords a greater drug loading capacity (6). However, despite their many benefits, NEs have issues with spreadability and skin retention due to their low viscosity (7). These drawbacks limit the therapeutic use of more conventional NEs for topical applications (8). The integration of NE in a gelling system has been proposed as a solution to this issue (9).

Nanoemulgel (NEG) formulations overcome the drawbacks of both NEs and hydrogels by combining both NE and gel properties. It is possible to introduce hydrophobic molecules into a hydrogel first by incorporating the compound into the oil phase of a NE and then introducing it to the gel base (10). Limitations of short scalp time for nanoemulsions can potentially be overcome by the gelling system that increases the viscosity of the NE; thus, enhancing contact time. Because of the homogeneous behavior and consistency of the hydrogel matrix, NEG have become popular dosage forms in recent years (11). In the present study, different MXD nanoemulsion formulations were prepared and the selected formulation was converted into a nanoemulsion-based gel (nanoemulgel) using Carbopol 934 as the gelling agent. This optimized formulation was fully characterized using various physical and *in vitro* performance tests.

MATERIALS AND METHODS

Minoxidil was obtained as a gift from Pharmaroya® pharmaceutical cosmetic industry (Istanbul, Turkey). Clove oil was purchased from SAC® - S.AMDEN and COMPANY 95 and 96/E, (Pakistan). Tween® 80 was bought from the Scharlab corporation (Barcelona, Spain). Propylene glycol was purchased from Merck® KGaA (Darmstadt, Germany). Absolute ethanol (analytical grade) was purchased from Scharlab corporation (Barcelona, Spain). Carbopol® 934 was

obtained from HiMedia lab (India).

Selection of oil phase

Solubility study of MXD in different oils

The solubility of MXD was measured in different oils. To conduct the test, clove oil (SAC® - S.AMDEN and COMPANY 95 and 96/E, Pakistan), castor oil (Lobachemie® lab reagents and fine chemicals, India), and oleic acid (Sigma-Aldrich, USA) were used. Five milligrams of MXD was added to glass vials containing 5 mL of each of the oils. These samples were then placed in an ultrasonic bath (Powersonic 410 HWASHIN ultrasonic cleaner R, Korea) for 15 minutes, followed by storage at room temperature for 24 hours before being inspected visually. The concentration of MXD was increased in each sample by adding 1 mg of MXD to the vials, and the procedure was repeated. After each iteration of the procedure all samples were inspected visually by observing the clarity and transparency of the solution. This technique was continued for each oil until there was evidence of MXD precipitation. Solubility of MXD in each oil was determined based on the maximum MXD in solution before precipitation occurred (5).

Determination of emulsifying efficiency of surfactant in different oils

To select the most appropriate oil phase for incorporation in nanoemulsion formulations, each oil was assessed for their ability to be emulsified by the selected surfactant, Tween® 80. The procedure used an aqueous titration method, which involved the addition of the oil drop by drop to a 10% v/v aqueous solution of Tween® 80. After each addition of the oil phase, the mixtures in the beakers were gently mixed with a magnetic stirrer until the mixture of the two phases remained clear and transparent. Samples were equilibrated at room temperature for 24 hours, followed by visual inspection. Addition of the oil phase was continued until turbidity appeared/evidence of phase separation occurred in samples after storage at 24 hours. (5).

Construction of pseudoternary phase diagrams (phase behavior study)

To obtain the NE areas and the precise concentrations of NE components, a pseudoternary phase diagram was constructed using an aqueous titration method. Tween® 80 and ethanol were used at different volume ratios to form what is known as Smix (surfactant:co-surfactant). Different ratios of Smix (1:1, 1:2, 1:3 and 2:1) were studied for the development of NEs. For each phase diagram, clove oil and S-mix were thoroughly mixed in separate beakers at various volume ratios (1: 9, 2: 8, 3: 7, 4: 6, 5: 5, 6: 4, 7: 3, 8: 2, and 9: 1), then the solvent system (DW/ PG at a ratio of 8.5:1.5) was added in a dropwise manner and titrated slowly at ambient temperature. After each addition of the aqueous phase, the mixtures in the beakers were gently stirred for 2 min. using a magnetic stirrer (Isotemp® fisher scientific, Korea) and allowed to equilibrate. Any changes in the mixture physical state from transparent to turbid were visually observed. CHEMIX (cxse 900) software was used to present the data as a triangle graph. Each axis in the triangle represents one of the component of the NE (oil phase, aqueous phase and Smix ratio) (12).

Preparation of MXD-loaded NE formulations

The MXD-loaded NEs were prepared initially by a low-energy method; then a high-speed homogenization technique was employed. Eight different formulations were prepared as shown in Table 1. 100 mg of MXD was accurately weighed as required for the preparation of 10 grams of formulation and it was dissolved in the Smix at its predetermined Tween® 80 and ethanol ratios by sonication for 20 minutes in an ultrasonic bath (Power Sonic 410 Copley Scientific, U.K). Then, the clove oil was added to the mixture and the whole mixture was stirred for 5 minutes at 700 RPM using a magnetic stirrer. This was followed by dropwise addition of a specified volume of the solvent system (DW+PG) with continuous stirring until a homogenous, clear, and transparent NE was obtained (13). Finally, the prepared NE was subjected to high-speed homogenization to achieve a stable NE, carried out using a high-speed homogenizer (Fisher Scientific

Table 1 Compositions of different MXD-loaded NEs.

	% w/w OF A COMPONENT OF NE					
Formulation	**Smix (S:Co-S) ratio**	**Smix (Tween80: Ethanol)**	**Oil (Clove oil)**	**Co-solvent (Propylene glycol)**	**Distilled water (DW)**	**Drug (MXD)**
NE-A1	1:1	40	5	8.25	45.75	1
NE-A2	1:2	40	5	8.25	45.75	1
NE-A3	1:3	40	5	8.25	45.75	1
NE-A4	1:4	40	5	8.2	45.75	1
NE-A 5	1:2	40	8	7.8	43.2	1
NE-A 6	1:2	40	10	7.5	41.5	1
NE-A7	1:2	35	5	9	50	1
NE-A8	1:2	45	5	7.5	41.5	1

PowerGen 125, USA) in a discontinuous mode. 10 ml of each prepared formula was processed by applying 3 consecutive cycles of 5 minutes on and 5 minutes off at 25000 RPM (14).

Characterization of MXD-Loaded NEs

Measurement of pH, electrical conductivity and light transmittance

The pH and electrical conductivity of all prepared NE formulations were measured using a pH meter (Isotemp® Fisher Scientific, Korea), and digital conductivity tester (Senz μSiemen, trans instrument, Singapore) respectively. The light transmittance was determined using UV/visible spectrophotometer (Labomed, Inc. USA) at 630 nm against DW as blank. One ml of each formula was made up to 10 ml with distilled water (DW) prior to measurement. All measurements were carried out in triplicate (15, 16).

Droplet size, size distribution and zeta potential of the prepared NE

The droplet size and droplet size distribution of all prepared NEs formulations were measured using a dynamic light scattering technique (DLS) using a particle size analyzer (Litesizer™ 500, Anton Paar, Austria). Zeta potential was measured by an electrophoretic light scattering technique (ELS) using a zeta potential analyzer (Litesizer™ 500, Anton Paar, Austria) by measuring particle speed in the presence of an electric field. Droplet size was presented as a mean hydrodynamic diameter (HDD) and droplet size distribution was presented as a polydispersity index (PDI) percentage. All measurements were carried out in triplicate (17).

Determination of entrapment efficiency

The entrapment efficiency (EE %) of the MXD-loaded NE formulations was determined by separation of unentrapped drug in each of the prepared formulations using ultrafiltration using 0.2 μm syringe filters. These samples were then diluted in a phosphate buffer solution (pH 7.4) to the required concentrations and the absorbance of MXD were determined by UV–visible spectrophotometer at the selected λ max. (The test was carried out in triplicate) (18).

EE % was calculated using Equation 1.

$$EE(\%) = \frac{\text{Quantity of API entrapped}}{\text{Total quantity of API added}} * 100 \qquad \text{Eq. 1}$$

Thermodynamic stability study

Stability testing was conducted according to International Conference on Harmonization (ICH) guidelines for climatic zone III region which pertain to local requirements for registration of pharmaceuticals for human use. All of the NE formulations were

stored in amber glass vials throughout the duration of the stability testing. Different thermodynamic stability tests were carried out on the NE formulations as outlined in the following sections.

Heating-cooling cycle

The NE formulations were subjected to six cooling and heating cycles at temperatures ranging from (4 to 45°C, RH 70%), with each temperature being maintained for 48 hours. After storage, the samples were visually examined for precipitation or phase separation.

Centrifugation

The formulations that remained stable after the heating-cooling cycle were centrifuged (Labofuge A, HERAEUS SEPTECH, Germany) for 30 minutes at 3500 RPM. After centrifugation, formulations that did not show any phase separation by visual assessment were subjected to a freeze-thaw cycle.

Freeze-thaw cycle

To check if there was phase separation, the formulations were subjected to three freeze/thaw cycles between -21°C and +25°C for 48 hours at each temperature (19). The samples were visually examined after the freeze/thaw cycle.

Transmission electron microscopy (TEM)

The morphology and size of the optimized MXD-loaded NE samples were characterized by transmission electron microscopy (TEM, Zeiss EM10C, Germany). The optimized formula was diluted with DW 100 times. One drop of diluted sample was transferred onto a carbon coated copper grid mesh 300, dried for 1 hour at room temperature and then measured by TEM at 100 kV (20).

Preparation of MXD-loaded NEG formulations (MXD-loaded NEG)

Carbopol® 934 was selected as the gelling agent. Carbopol® 934 solutions at different concentrations (1% w/v, 2% w/v and 3% w/v) were prepared by dissolving the required weight of Carbopol® 934 in (10 ml) DW stirring constantly at moderate speed using a magnetic stirrer. After complete dispersion, the dispersed solution was stored in a dark place for 24 hours to allow the polymer to fully hydrate, and to remove any entrapped air bubbles. Then, the pH was adjusted to 5.5 by adding a few drops of triethanolamine (TEA) to produce a clear and transparent gel (21).

Finally, three different MXD-loaded NEG formulations were prepared, as shown in Table 2**,** by incorporating the optimized MXD-loaded NE formulations with the gels previously prepared at different concentrations. The mixing was in a ratio of 1:9 of NE to gel with a constant stirring at optimum speed using a magnetic stirrer until a uniform and homogeneous NEG was obtained.

Characterization of MXD-Loaded NEG formulations

Measurement of pH, spreadability and viscosity

1 g of each MXD-loaded NEG formulation was

Table 2 Compositions of different MXD-Loaded NEG

	% w/w of a component of NEG						
Formulation	**Smix (S:CO-S) ratio**	**Smix (Tween80 : Ethanol)**	**Oil (Clove oil)**	**Co-solvent (Propylene glycol)**	**Distilled water (DW)**	**Drug (MXD)**	**Carbopol 934**
NEG-A2X	1:2	40	5	8.25	45.65	1	0.1
NEG-A2Y	1:2	40	5	8.25	45.55	1	0.2
NEG-A2Z	1:2	40	5	8.25	45.45	1	0.3

accurately weighed and diluted up to 10 ml with DW. The pH of the NEG formulations was determined using a digital pH meter (EcoTestr pH 2, Singapore) (22).

The spreadability test was conducted on all MXD-loaded NEG formulations using a wooden block and glass slide apparatus. The device consisted of a wooden block with a pulley attached to one end. Two glass slides of the same dimensions were employed in this device, and spreadability was determined based on "slip" and "drag" properties of the NEG (23). Two grams of each prepared formula were placed on the surface of a glass slide that was already fixed on the wooden block. The NEG samples were then sandwiched between this slide and an upper glass slide. A weight of 100 g was placed on the surface of the upper slide for 5 minutes to expel air and to produce a consistently thin film. The upper glass plate was then dragged with a 20 g weight using a string attached to the hook and the time (in seconds), which was needed for moving the upper slide 7.5 cm was recorded. Better spreadability is indicated by a shorter interval (21).

Spreadability (S) was calculated using Equation 2.

$$S = \frac{M * L}{T} \qquad \text{Eq. 2}$$

Where;
S = spreadability, M = weight tied to upper slide (g), L = length of glass slide (cm), T = time taken by the slide to move the distance (sec.)

The viscosities of the developed NEG formulations were determined using a Brookfield DV-II viscometer fitted with a spindle cone plate number CP-41z, which was immersed in each sample of the prepared formulations and rotated at different speeds (0.1, 1 and 5 RPM). The viscosity was measured at 22.5 ±2°C in triplicate (24).

In vitro drug release

The in vitro drug release test was conducted using a USP dissolution apparatus type II (paddle apparatus) (Copley scientific, UK) at a rotation speed of 50 RPM and temperature maintained at 37±0.5°C using a dialysis bag (Molecular cut off: 12000-14000 D). The *in vitro* drug release was studied for MXD-loaded NEG formulations, optimized MXD-loaded NE formulations, standard alcoholic solution and a marketed MXD solution (Hairgrow® 2%, Dar aldawa, Jordan).

The tested samples were placed in dialysis bags. The bags were closed at both ends, attached to the dissolution apparatus paddle using a cotton thread, and immersed completely in 200 ml phosphate buffer solution (0.2M) at pH 7.4. Aliquots of 5 ml were withdrawn at intervals of 5 minutes, 15 minutes, 0.5, 1, 2, 3, 4, 6 and 7 hours. Each aspirated sample was replaced by an equal volume of phosphate buffer pH 7.4 at 37°C. Concentrations of MXD were determined using a UV/Vis spectrophotometer (Labomed, Inc. USA) at the λ max of the drug; 288 nm. The percentage of cumulative drug release was calculated and plotted against time (25). (Each test was carried out in triplicate).

Various kinetic models and equations were used to determine the release kinetic of MXD in which the cumulative release data was fitted into zero order kinetic, first order kinetic, Higuchi model and Korsmeyer and Peppa's model. The kinetic model was chosen based on the highest correlation coefficient (r2) (26).

Ex vivo permeation study

The *ex vivo* skin permeation study protocol was approved by the institutional animal care and use committee at the College of Veterinary Medicine, University of Mosul with approval number (UM. VET.2021.004). The study was carried out using a Franz diffusion cells with effective diffusional area 0.64 cm^2 and volume 5 ml receiver chamber capacity. The skin from Swiss albino rats weighing 200 ± 10 grams was used in this study and the full thickness of fresh skin was surgically removed from abdomen and subcutaneous tissue was also removed then the hair was removed by hair clipper. Visual inspection by

light microscopy (Olympus CX21, Japan) was used to confirm complete hair removal and as a macroscopic assessment of skin integrity.

Skin samples were immersed in phosphate buffer solution pH 7.4 to achieve good hydration. Each skin sample was placed in the Franz diffusion cell (Permegear, inc., USA) and fixed between the donor and receiver chambers, with the stratum corneum (SC) side facing the donor chamber. The receiver chamber was filled with phosphate buffer solution pH 7.4. and kept at constant temperature 37 ± 0.5°C with continuous stirring at 260 RPM for 7 hours using a hot plate magnetic stirrer (Labnet International, Inc. Mexico).

The study was carried out on the optimized MXD-loaded NEG formulation and marketed solution (Hairgrow® 2%, Dar aldawa, Jordan). The tested samples were introduced directly onto skin in the donor chamber. Samples of 0.3 ml were withdrawn at intervals of 0.5, 1, 2, 4, 6, 8 and 24 hours, and each aliquot removed was replaced by equal volumes of phosphate buffer solution pH 7.4. The samples were adequately diluted and examined by a UV/Vis spectrophotometer at the λ max of the drug (27).

Permeation parameters analysis

The cumulative amount of MXD that permeated per square centimeter through the abdominal rat skin (Q, µg/cm2) was measured and plotted *versus* time. The permeation rate (flux) at steady state (Jss) was measured from the slope of the plot which is generated by plotting the cumulative amount of MXD permeated per unit area versus time at the steady-state condition. The permeability coefficient (Kp) was measured by dividing the permeation rate at steady state of MXD over the initial drug concentration, which was applied to the donor compartment (Co) as shown in Equation 3.

$$Kp = \frac{Jss}{Co} \qquad \text{Eq. 3}$$

Where;

Kp = permeability coefficient, Jss = steady-state flux, Co = initial concentration of MXD in the donor compartment.

Enhancement ratio (Er) was calculated by dividing the Kp of the optimized MXD-loaded NEG formulation by the Kp of the marketed solution as a control and calculated using Equation 4 (28).

$$Er = \frac{Kp\ of\ formulation}{Kp\ of\ control} \qquad \text{Eq. 4}$$

Stressed Stability study

The optimized MXD-loaded NEG formulation was stored in an amber glass vial and was exposed to three different temperatures at 6 ±2°C (in the refrigerator), 25 ±2°C (at room temperature), and 40 ±2 °C /75 % RH (stress condition) for up to 90 days. The formulation was evaluated for changes in color, homogeneity, pH and electrical conductivity after storage for 1, 2, and 3 months (29).

Statistical Analysis

Every experiment was carried out three times (n=3). Data were analyzed and expressed using GraphPad≤ Prism 9.2.0. and Microsoft Office Excel 2016. Numeric data were expressed as (Mean ± SD). One-way ANOVA test/Tukey's Test for Post-Hoc Analysis and unpaired t-test were used for comparing values of the mean for the various groups. The statistical significance was ascertained at (P≤0.05).

RESULTS AND DISCUSSION

Selection of oil phase

Solubility study of MXD in different oils

All the excipients considered for use in the nanoemulsion formulations are safe, pharmaceutically acceptable and are non-irritant to the skin. A precise balance of components is necessary for nanoemulsion formulations to have the requisite product performance in terms of delivery and stability. Drug loading is

considered as one of the most important factors in the selection of components and in determining a formulation approach.

The results are shown in Table 3. Results from the MXD oil solubility study showed that more drug loading was possible in oleic and clove oil, which showed increased solubility of MXD, than castor oil. The ultimate choice of clove oil was based on data from both the solubility and the emulsification efficiency study, as well as literature data, indicating its potential beneficial effects on hair (30).

Table 3 Saturation solubility of MXD in different oils

OIL TYPE	SOLUBILITY mg/ml
Castor oil	1
Clove oil	17
Oleic acid	18

Determination of emulsifying efficiency of surfactant in different oils

The selected oil phase for a NE formulation should have the ability to be dispersed efficiently into fine droplets in the selected surfactant, at the concentration used in the formulation (in this case a 10% (v/v) Tween® 80 solution), without any signs of phase separation. The results for the emulsifying efficiency of the surfactant with the three potential oil phases are shown in Figure 1. Solubility of the different oils in 10% (v/v) Tween® 80 solution was in the order: Clove oil > oleic acid > castor oil. A 10% (v/v) Tween® 80 solution dispersed up to 28.43 ±0.42% of clove oil, 16.37 ±0.38% of oleic acid and 9.17 ±0.35% of castor oil.

Tween® 80 shows the greatest emulsification for clove oil, and this might be due to the high emulsification efficiency of Tween® 80 on eugenol, which is the major component in clove oil. This is consistent with work carried out by Nagaraju *et al.* (31), who reported on using Tween® 80 in the preparation of clove oil-based NEs. Results from this study, and reports in the literature, show that clove oil can be effectively dispersed with Tween® 80, at relatively high concentrations of oil, without phase separation. Based on this, clove oil was selected as the oil phase for the fabrication of prototype MXD-loaded nanoemulsions.

Construction of pseudoternary phase diagrams (phase behavior study)

In the absence of MXD, pseudoternary phase diagrams were constructed to identify the NE region (monophase area) and to optimize the concentration of oil, surfactant, and co-surfactant in NE formulations by using Tween® 80 as a surfactant, ethanol as a co-surfactant, and PG and DW as the solvent. Four diagrams were constructed using the aqueous titration method, and by varying the volume ratio of surfactant to co-surfactant (S:CO-S) in what is called Smix and the diagrams named (1:1, 1:2, 1:3 and 2:1).

The shaded area in the pseudoternary phase plot represents the area of NEs, whereas the unshaded area shows the emulsion area. The plot with a larger shaded region suggests that the produced NEs have ideal nano-emulsifying efficiency and good interaction between the Smix, oil, and aqueous phase (13). Tween® 80 has an HLB value of 15, indicating that it is a hydrophilic surfactant. These surfactants are more soluble in the aqueous phase, favoring the formation of o/w NEs according to Bancroft's rule (32).

The pseudoternary phase diagram plots for different Smix volume ratios of 1:1, 1:2,1:3 and 2:1 are shown in Figure 2. According to the results obtained from each diagram, the largest shaded area (NE area) was shown in the 2:1 plot. This result might be due to an increase in the concentration of surfactant to co-surfactant in Smix 2:1 relative to 1:1, which causes a great improvement in oil solubilization. Furthermore, at Smix 1:2 and 1:3 ratios, an increase in co-surfactant concentration with a corresponding decrease in surfactant concentration resulted in a reduction in the NE area. This result is similar to that found in previously reported work by Khames *et al.*, who prepared an eplerenone NE as an oral drug delivery system with improved bioavailability

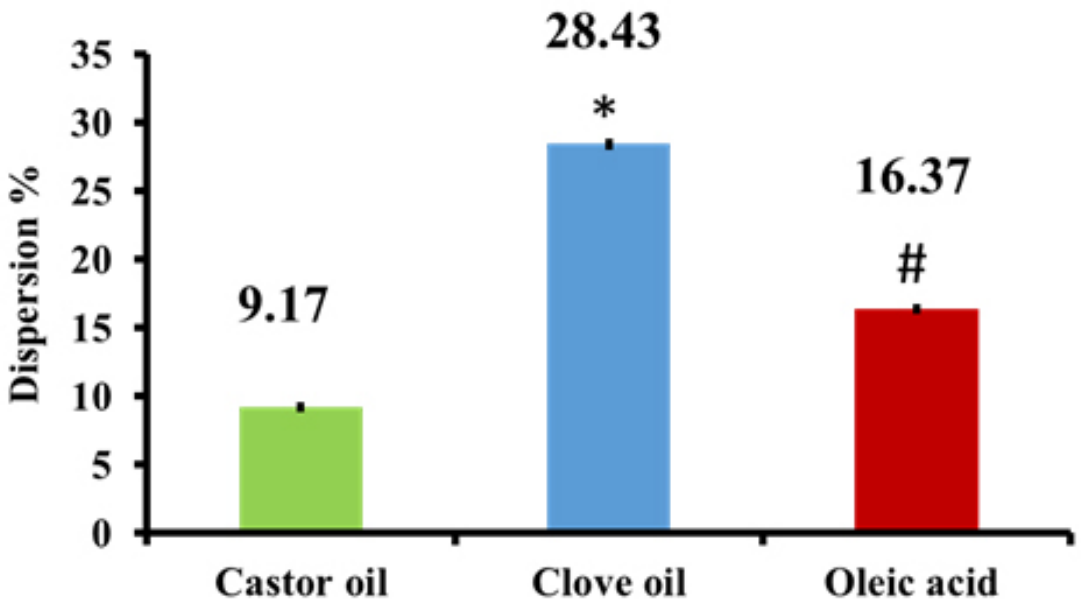

Figure 1 Solubility of different oils in 10% Tween 80® solution. Data are expressed as mean ±SD, *# P≤0.05.

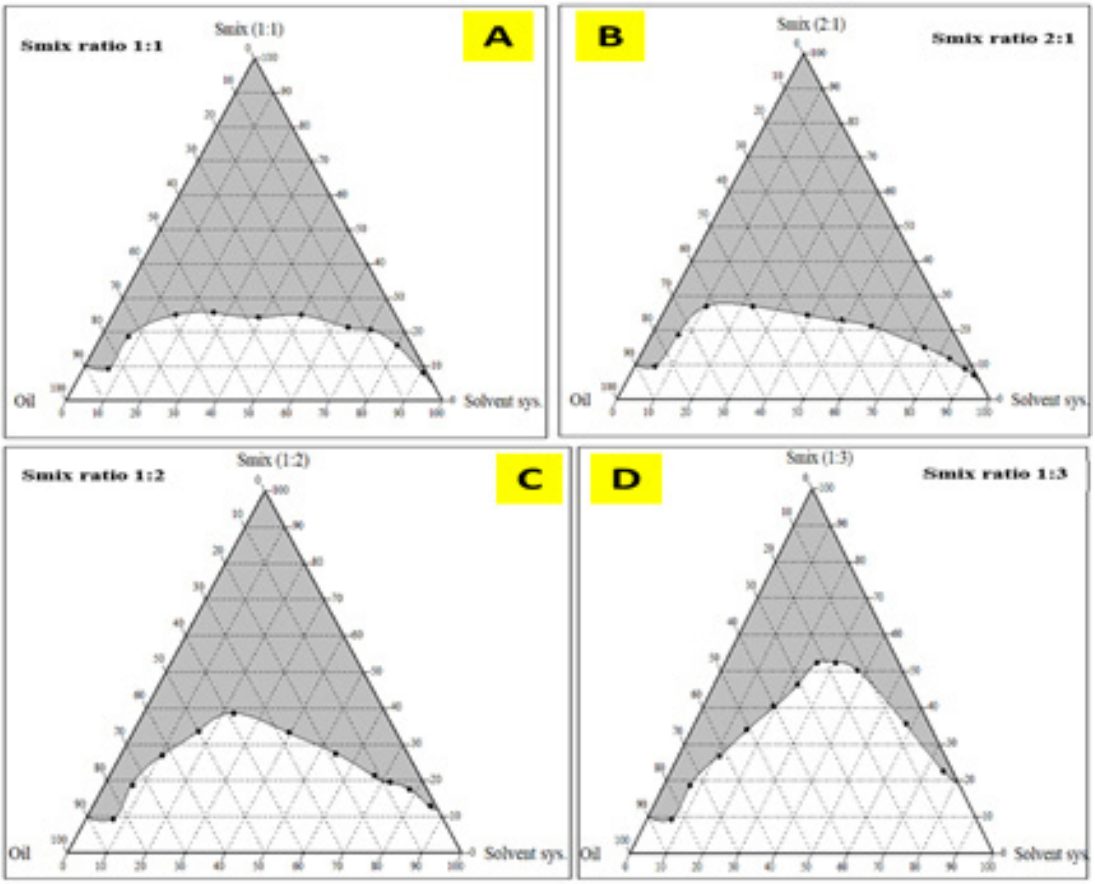

Figure 2 Pseudoternary phase diagrams. The diagrams showed (o/w) NE (shaded area) regions of clove oil (oil), Tween® 80 (surfactant), ethanol (co-surfactant) at different Smix ratios: (A) Smix 1:1, (B) Smix 2:1, (C) Smix 1:2 and (D) Smix1:3 at 25°C.

(33). Based on these results, the remaining formulations were prepared from all the NE shaded areas that are shown in all the diagrams (Figure 2).

Characterization of MXD-loaded NE

Measurement of pH, electrical conductivity and light transmittance

The pH values of the prepared MXD-loaded NE formulations are shown in the Table 4. The pH values were found to be between 7.2 and 7.4. These values indicated that all NE formulations have neutral pH and could be applied safely to the skin without any irritation due to physiological compatibility with the skin pH (34). For o/w emulsions, the conductance value is greater than 10 μS/cm, while for w/o emulsions the conductance value is less than 10 μS/cm. According to the results presented in Table 4, all the prepared NE formulations were of the o/w type, because all eight formulations had conductivity values of greater than 10 μS/cm (35). The conductivity value for formula NE-A3 was the least among the formulations due to the higher ratio of ethanol in the Smix. In comparison, the NE-A4 formulation had the highest value of conductivity, which might be due to the lowest ratio of ethanol in the Smix. The explanation behind the significant difference (P≤0.05) between NE-A3 and NE-A4 formulations might be that increasing the concentration of ethanol generates more hydrogen bond interactions with water, leading to a reduction in the ion speed in the solution, and consequently lowers the electrical conductivity (36).

Table 4 pH, conductivity and transmittance % of NE formulations

FORMULATION	pH	CONDUCTIVITY μS/cm	TRANSMITTANCE %
NE-A1	7.4±0.1	39.17±1.33	99.18±0.6
NE-A2	7.4±0.04	31.67±2.88	99.17±0.2
NE-A3	7.3±0.1	25.67±2. 66	98.78±0.9
NE-A4	7.2±0.05	43.17±2.04	99.19±0.4
NE-A5	7.3±0.06	37.2±1.72	98.62±0.13
NE-A6	7.2±0.06	38.5±2.07	98.10±0.57
NE-A7	7.4±0.011	38.0±1.7	98.77±0.25
NE-A8	7.4±0.08	40±0.9	98.95±0.47

Mean ±SD, n=3

The transmittance percentage of a NE demonstrates the transparency of the systems. The values of transmittance for all eight formulations are shown in Table 4. The percentage of transmittance of the NEs was in the range of 98.10 ±0.57 to 99.19 ±0.4.These results confirm that all formulations were clear, transparent, and easily transmitted the light due to their nano-size droplets (37).

Measurement of droplet size and polydispersity index and zeta potential of the prepared NE formulations

The measurement of the hydrodynamic diameter (HDD) of the MXD-loaded NEs was conducted and the experimental results are shown in Figure 3. To study the effect of Smix ratio on HDD, a comparison was made between NE-A1, NE-A2, NE-A3 and NE-A4, where the concentration of oil and co-solvent were constant. Figure 3 (i) showed that NE-A1, NE-A2, and NE-A3 formulations were in the nanometer size range, but NE-A4 had a larger droplet size. Interestingly, the NE-A2 formula, with Smix ratio (1:2), achieved the lowest HDD, which is statistically different (P≤0.05) from other formulations. The small mean HDD in NE-A2 may be attributed to penetration of the co-surfactant molecules into the surfactant film. This may minimize the interfacial surface, lower the radius of curvature of droplets, and produce transparent systems (38).

Results also showed that NE-A4 has the largest HDD and this may be due to change the ratio of Smix from (2:1) to (1:2). By increasing the Tween® 80 concentration in relation to ethanol, the mean HDD increased significantly from 14.62 nm ±1.36 to 512.3 nm ±150.53 (P≤0.05). Droplet size was increased as surfactant concentration increased, possibly due to the depletion-flocculation mechanism of the adsorbed surfactant. As surfactant concentration rises, it forms micelles in the continuous phase rather than orienting on particle surfaces. This results in moving the continuous phase between some droplets, and when this phase is fully depleted aggregation occurs, and the

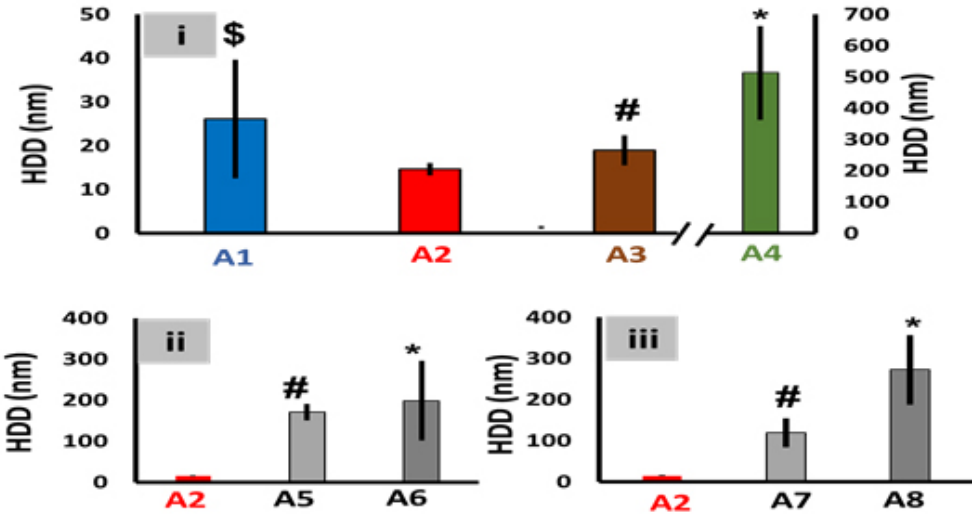

Figure 3 Hydrodynamic diameter (HDD) for the eight formulations. HDD for MXD-loaded NE formulations with different Smix ratios (i), HDD for formulations with different ratios of oil (ii) HDD for formulations with different concentrations of surfactant (iii). Data expressed as mean±SD, *$# P≤0.05.

HDD increases (39).

To study the effect of oil concentration on HDD, a comparison was made between NE-A2, NE-A5 and NE-A6 formulations. The results, (Figure (3) (ii), show that the NE-A2 formulation which has a lower concentration of clove oil than NE-A5 and NE-A6, has a significantly smaller average HDD (P≤0.05) (14.62 nm ±1.36). Alternatively, increasing the oil concentration to 8% (v/v) in formulation NE-A5, produced a larger HDD (171.03 nm ± 20.28).

A further increment of clove oil concentration from 8% to 10 % (v/v) in formula NE-A6, generated NEs with significantly higher HDDs (198.50 nm ±97.44) (P≤0.05). This implies that the greater the oil content, the larger the mean HDD. These findings were consistent with the results of Yuan *et al.*, who found that an increase in the concentration of the oil phase of a NE results in a larger HDD. This effect is due to the expansion of the oil droplets in the NE and might also be due to the concurrent reduction in the Smix ratio (40).

In contrast, a comparison was performed between NE-A2, NE-A7, and NE-A8 to examine the influence of Smix concentration on HDD. Figure 3 (iii) demonstrated that the NE-A2 formula has an optimum Smix concentration of 40% (v/v). By reducing the Smix concentration to 35% (v/v) in the NE-A7 formulation, the HDD was substantially increased from 14.62 nm ±1.36 to 118.86 nm ±35.71 (P≤0.05). When the emulsifier concentration at the oil-water interfacial layer is insufficient to completely cover the surface of the drops, coalescence and flocculation of droplets occurs and the size of the droplets is increased (121). When the concentration of Smix was increased from 40% to 45% (v/v), as in formulation NE-A8, the mean HDD significantly increased from 14.62 nm ±1.36 to 272.53 nm ±84.68 (P≤0.05).

The polydispersity index (PDI) measures the homogeneity of the nano-sized droplets. PDI values range between 0.0 and 1.0. The closer the PDI to zero, the more homogeneous the distribution of the nano-sized globules are. Consequently, the lower the homogeneity of the droplets in the formulation, the greater the PDI (41). Figure 4 represents the results of the PDI of all the prepared MXD-loaded NEs. In all cases the PDI was found to be less than 0.3, which indicates a homogeneous distribution of nano-sized droplets within the NE which improves the physical stability of the system (42).

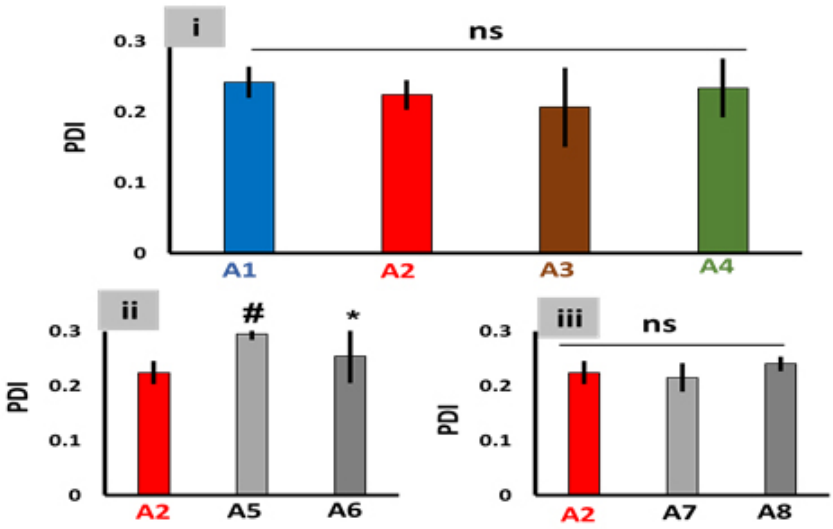

Figure 4 Polydispersity index (PDI) of the eight formulae. The PDI for formulae with different Smix ratios (i), PDI for formulations with different concentrations of oil (ii) PDI for formulations with different concentrations of Smix (iii). Data expressed as mean±SD, *# P≤0.05. ns stand for – not significantly different.

The droplet size distribution analysis of the MXD-loaded NE formulation is shown in Figure 5. Only formula NE-A2 and formula NE-A3 had mono-modal distributions with a single peak, which indicates a homogeneous droplet distribution and less liability for stability problems. The other formulations have bimodal and multimodal distributions with two or three peaks, which indicates the presence of aggregated droplets. These multimodal and bimodal distributions are most likely caused by oil droplet flocculation, which results in a larger droplet size. This could encourage the coalescence of small droplets into larger ones, which reduces the stability and increases the droplet size of the NE. These findings substantiate the importance of using multiple methods such as, the mean droplet size Figure 3, polydispersity index Figure 4 and size distribution analysis to better understand particle size distribution behavior of nanoemulsions (43).

Zeta potential is an essential characteristic that describes physical stability of NEs. Formulations having a zeta potential range equal to or greater than ± 30 mV are considered as an electrically stable systems that are kinetically stable (44).

The values of zeta potential of all formulations are presented in Figure 6. The values of zeta potential in all the prepared NE were negative indicating negatively charged particles. This behavior has been reported previously by Alhakamy *et. al.* who found that nanoemulsions containing Tween® 80 had negative zeta-potential values (45). Their explanation was this could be due to the presence of free fatty acid impurities in this non-ionic surfactant. In the current work the negative surface charge could also be attributed to the presence of anionic groups of fatty acids and glycols, which are present in the clove oil and co-solvent (45). The presence of a negative charge on the surface of NE droplets encourages them to penetrate the skin (46). Similar findings were observed by Khurana *et al.*, who developed stable, negatively charged, meloxicam-loaded NE gels containing caprylic acid as an oil phase (7).

Although the zeta potential of the chosen formulations is relatively low, it is important to note that Tween® 80 has a large molecular weight, and it acts through steric stabilization rather than electrostatic stabilization. Nonionic surfactants, such as Tween® 80, adhere to nanoscale droplets and, while this causes a reduction in the zeta potential, they maintain stability in o/w NEs by forming a hydrated layer on the lipophilic particle

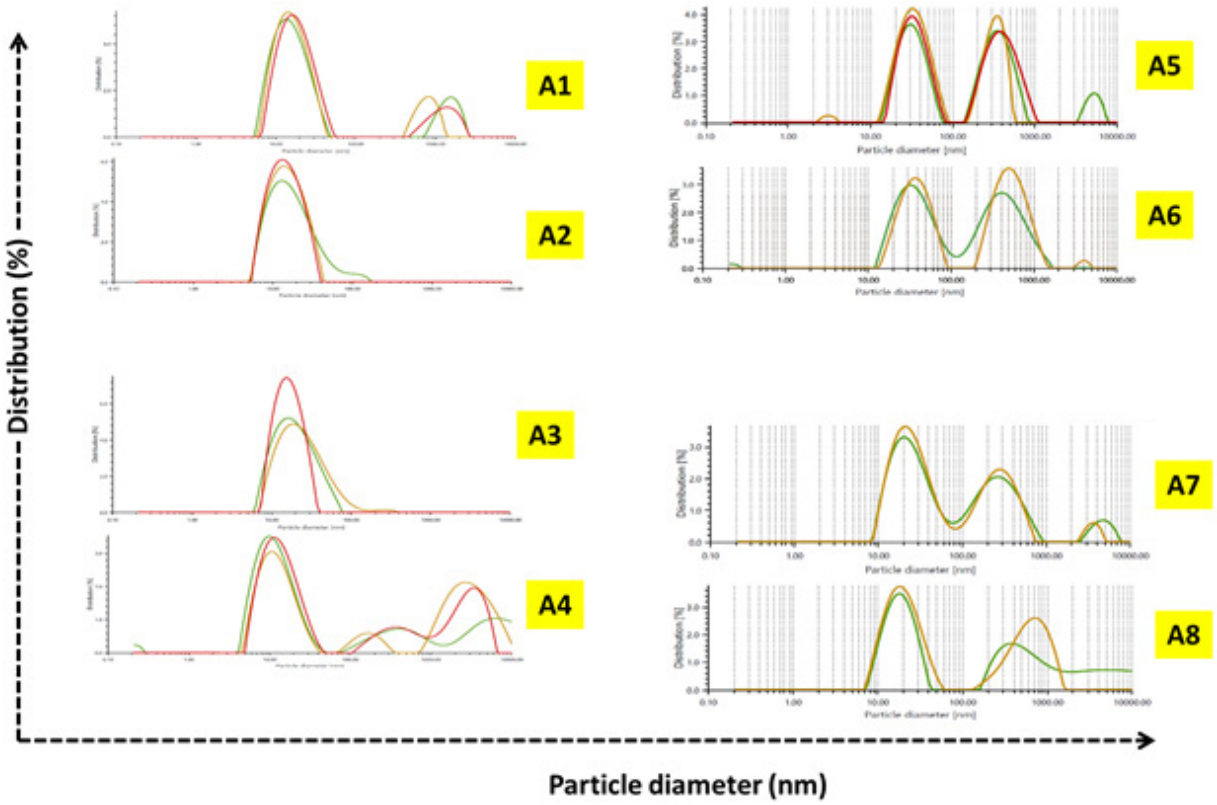

Figure 5 Droplet size distribution of NE formulations (The different colors represent the repeats of the reading of each formulation).

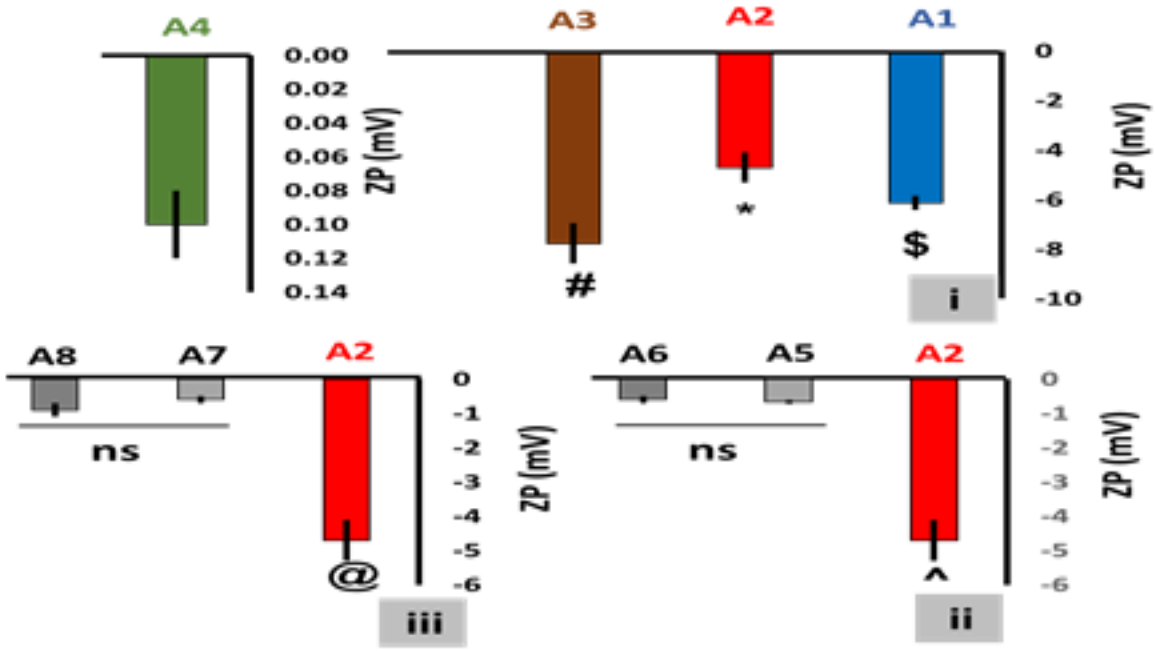

Figure 6 Zeta potential (ZP) representing the eight formulations (i) The ZP for formulations of different Smix ratio (ii) ZP for formulations with different oil concentrations (iii) ZP for formulations with different Smix concentrations. Data expressed as mean±SD, *$#^@ P≤0.05.

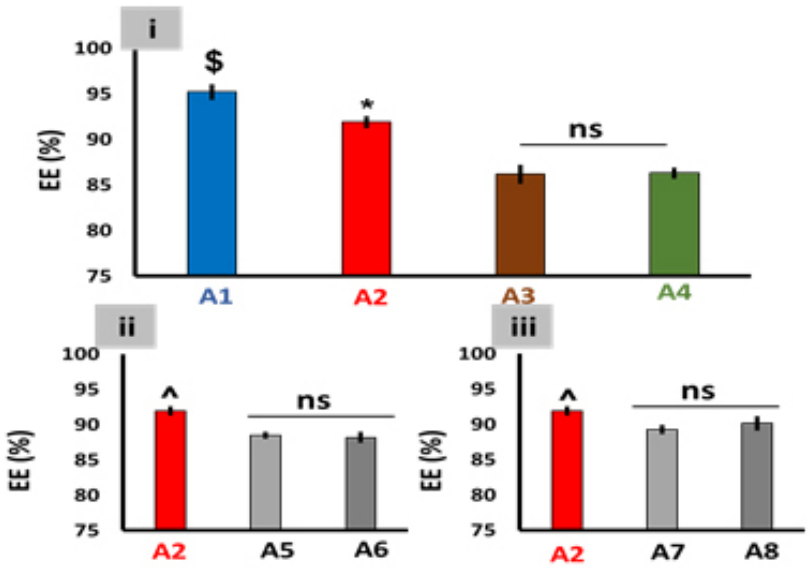

Figure 7 Entrapment efficiency percentage (EE%) of the eight nanoemulsion formulations. The highest entrapment efficiency results were recorded for formulations NE-A1 and NE-A2. (i) EE% for NE formulations with different ratios of Smix (ii) NE formulations containing different oil concentrations (iii) formulations of different Smix concentration were separately shown. Data expressed as mean±SD, $^* P≤0.05

(47).

Determination of entrapment efficiency

The amount of drug incorporated/encapsulated in the NE is referred to as the entrapment efficiency. The entrapment occurs due to the hydrophobic interaction between the drug and the oil droplets.(48). The results shown in Figure 7 depict the percentage drug encapsulation efficiency of all MXD-loaded NE formulations. The amount of MXD entrapped differed, ranging from 95.2±0.84% to 85.92±0.54 % with the drug entrapment varying by up to ~9% between the formulations. The entrapped fraction of MXD was potentially high, with the highest entrapment percentage observed in formulations NE-A1 and NE-A2.

There was a significant difference between NE-A1 and NE-A2 entrapment efficiency; however, the difference was considered relatively small, and when other investigated characteristics were taken into consideration, NE-A2 was considered superior to NE-A1 (see later section).

Thermodynamic stability study

Different tests, including heating-cooling cycle, centrifugation and freeze-thaw cycle tests were performed on all the prepared formulations NE-A1 through to NE-A8. All of these MXD-loaded NEs successfully passed this thermodynamic stability protocol with no signs of phase separation, creaming, cracking, or drug precipitation (49). The results showed that all the preparations had good physical consistency and stability.

Selection of optimized NE formulation

The selection of the optimized NE formula, that would undergo more extensive testing, was made based on several criteria, which included: having the smallest droplet size, having an acceptable polydispersity index (PDI), as well as giving the highest zeta potential (ZP) along with high entrapment efficiency. Consideration of all characterization results highlighted NE-A2 with Smix ratio (1:2), 5% oil concentration and 40% Smix concentration, was the most optimal formulation. NE-A2 has the lowest droplet size of 14.62 nm ±1.36, the lowest PDI of 0.22 ±0.021, an acceptable zeta potential

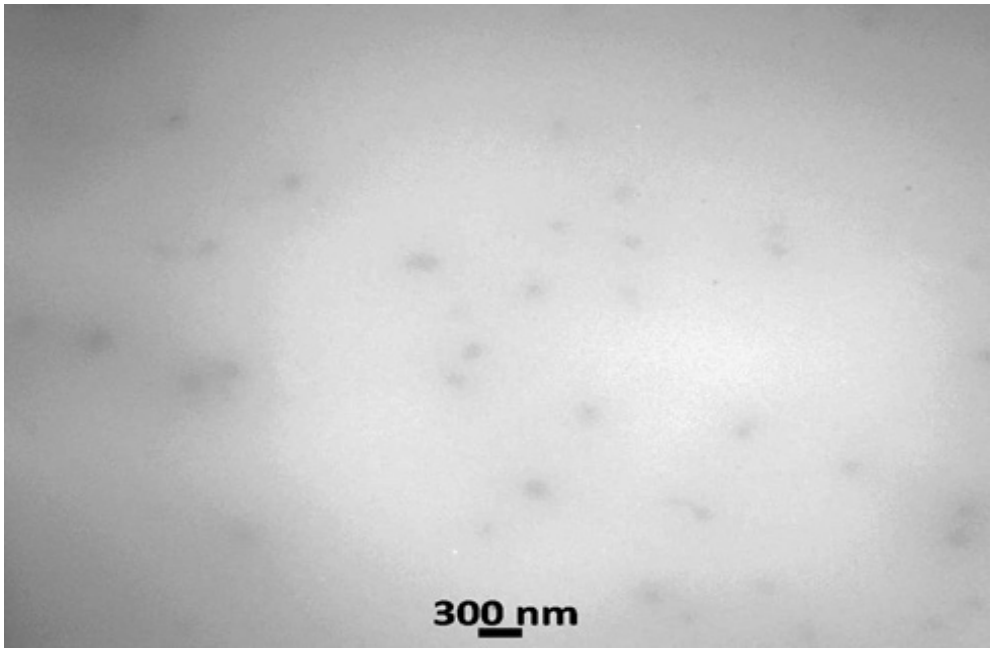

Figure 8 Photomicrographic representation of TEM of the selected MXD-loaded NE formula (NE-A2)

of - 4.7 ±0.6 and the high entrapment efficiency of 91.2 ± 0.31, compared with other formulations.

Transmission electron microscopy (TEM)

The optimized MXD-loaded formulation (NE-A2) was evaluated using TEM to characterize the droplet size and morphology. The photomicrograph is shown in Figure 8. TEM results show discrete spherical droplets with a homogeneous and uniform size that appeared to be less than 100 nm.

Moreover, this microscopic result supports our findings in the reported droplet size analysis, which was conducted using the dynamic light scattering technique (DLS). In addition, the result is consistent with a previous study reported by Kumar et al., (50).

Characterization of MXD-loaded NEG Formulations

Measurement of pH, spreadability and viscosity

The pH values of the developed MXD-loaded NEG formulations are shown in Table 5. All were observed to be between a pH range of 5.8 ± 0.05 to 6.2 ± 0.1. This pH range is acceptable for topical formulations and is not associated with adverse effects such as skin irritation. The results are similar to with previous literature (Soliman et al.,) in which NEG formulations were prepared with pH values from pH 5.5 to 6.4 (24).

Table 5 pH, spreadability and viscosity of the prepared NEG formulations

FORMULATION	pH	SPREADABILITY g.cm/s	VISCOSITY (cP)
NEG-A2x	6.2±0.1	24.3±0.67	93.3±16.64
NEG-A2y	6±0.08	21.6±0.73	492±87.81
NEG-A2z	5.8±0.05	18.4±0.89	----

Mean ±SD, n=3

The spreadability values for prepared NEG formulations ranged from 18.4 ±0.89 to 24.3 ±0.67 g.cm/s and there were significant differences between the three formulae (P≤0.05). According to these results, the formula NEG-A2y showed optimum spreadability 21.6 ±0.70 g.cm/s and indicated that the NEG was easily spreadable with a minimal amount of shear. This finding agreed with the result of work conducted by Dadwal et al (21). The results showed that the viscosity values were 93.3 ±16.64 cP and 492.0 ±87.81cP for NEG-A2x and NEG-A2y, respectively and there was a

significant difference between these two formulations (P≤0.05). It was noticed that the viscosity of NEG-A2z was not determined, because this formulation had a high viscosity. It was observed that NEG-A2y has the optimum viscosity for NEG to be applied topically and this result was similar to a previously reported result by Bhattacharya *et al.* (51).

in vitro drug release

For a topical medicinal product to be effective, the drug should first be released from the vehicles before partitioning into, or absorbed by, the skin during the biological permeation process. Assessing *in vitro* drug release is a useful surrogate for assessing drug skin penetration (52). The *in vitro* drug release profile was determined to evaluate the release of MXD from the optimized MXD-loaded NE formulation (NE-A2) and all NEG formulations in comparison to the alcoholic standard solution (Minoxidil 1% in ethanol solution) and marketed solution in phosphate buffer (0.2M) solution pH 7.4.

The cumulative *in vitro* drug release profile of MXD from six different formulations are presented in Figure 9. The results demonstrate that both the optimized MXD-loaded NE formulation (NE-A2) and the alcoholic standard solution showed around 99% cumulative drug release in 420 minutes. However, there is a reduction in the cumulative release profile of the marketed solution and the NEG formulations (NEG-A2x, NEG-A2y, and NEG-A2z).

The optimized MXD-loaded NE formulation (NE-A2) had similar cumulative release to that of the alcoholic standard solution and was greater than the marketed solution at 420 minutes under the same testing conditions. A contributing factor to this could be the fact that NE formulations have much smaller particle sizes, in the nano-size range, providing more surface area and interfacial area for dissolution (13).

To study the effect of different Carbopol® 934

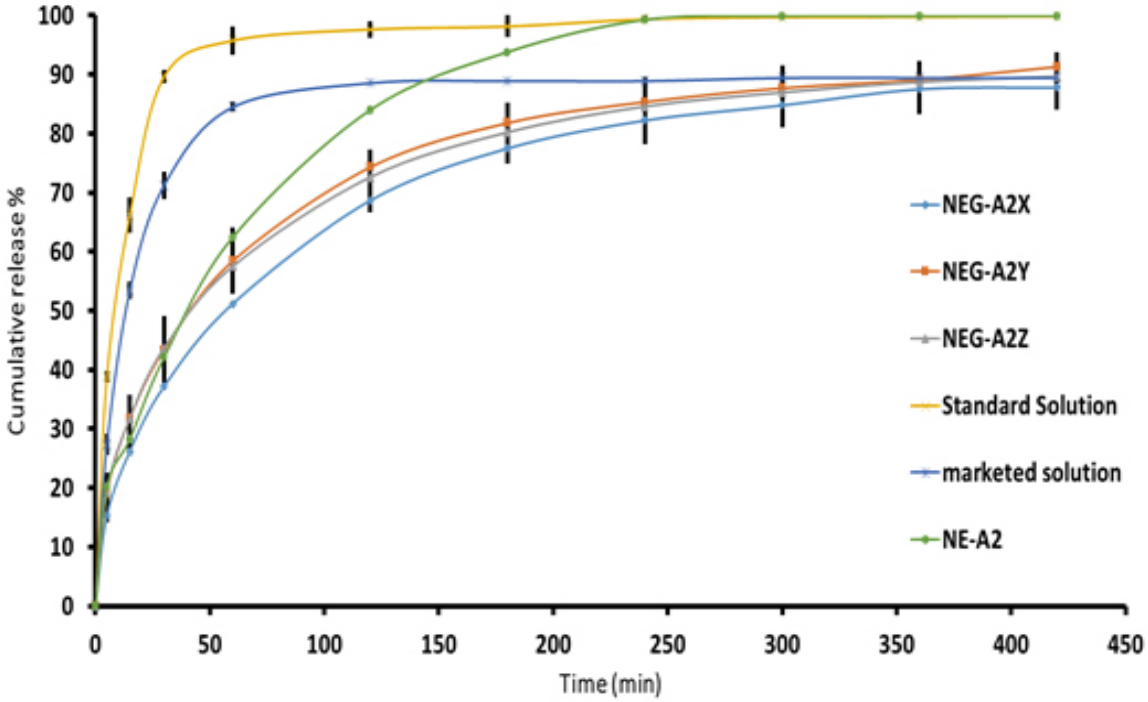

Figure 9 Cumulative release profile of different formulations. Six samples were tested (NEG-A2X (1%w/v Carbophol® 934) , NEG-A2Y (2%w/v Carbophol® 934), NEG-A2Z (3%w/v Carbophol® 934), Marketed solution, standard solution and NE-A2). Data expressed as mean±SD.

concentrations on the cumulative drug release profile, a comparison was made between three formulations containing different amounts of this excipient (NEG-A2x 1% w/v Carbopol®, NEG-A2y 2% w/v Carbopol® 934, and NEG-A2z 3% w/v Carbopol®). The results shown in Figure 9 highlight delayed drug release profiles for all nanoemulsion gel (NEG) formulations compared to the nanoemulsion (NE-A2) and the marketed product. In the group of NEG formulations there is no significant difference ($p<0.05$) between the cumulative drug released. Increasing the concentration of Carbopol® induced a slight change, but statistically non-significant effect, on total drug release and the overall release profiles were similar in all three NEG formulations. It has been reported that different concentrations of gelling agent in the gel matrix of nanoelmusion gels causes a decrease in the rate of release (49). No differentiation in the total release, and minimal changes to the overall release profile were observed in the current study indicating that there is no benefit in selecting one concentration of Carbopol® over the others in this case. This is likely due to the low, and very similar concentrations of Carbopol®, which delayed release to the same extent. In summary, the inclusion of the gelling agent, Carbopol®, in the NE formulation resulted in a delayed release profile with lower total drug release at 420 minutes. No differences in drug release profiles were observed between the three NEG systems. Selection of a NEG to study further was somewhat empirical with NEG-A2y being selected based on it showing a marginal increase in cumulative release (91.30 ±2.51 % at 420 minutes.) *versus* the other two NEGs.

Mathematical modeling of drug release

Different kinetic models (zero order kinetic, first order kinetic, Higuchi model, and Korsmeyer-Peppa's model) have been used to describe the kinetic release of MXD from the all the prepared formulations.

Release kinetic data of MXD from different formulations phosphate buffer solution pH 7.4 are shown in Table 6. The data analysis illustrates that the marketed solution and NEG formulations have the highest regression coefficient (r^2), which fits with Higuchi's model. This suggests that diffusion is involved in the release mechanism of MXD from the drug delivery system (DDS). However, the optimized MXD-loaded NE formula (NE-A2) and alcoholic standard solution follow the first order kinetics in which the rate of drug release is directly proportional to the concentration of drug (26).

Ex vivo permeation study

The amounts of MXD that permeated through the excised rat skin model for the optimized MXD-loaded NEG formula (NEG-A2y) and the marketed solution are shown in Figure 10. The cumulative amount of MXD permeating through the skin over 24 hours from the NEG-A2y formula was 961.97 ±4.77 and was significantly ($P\leq0.05$) higher than that from the marketed solution 398.24 ±10.03.

The values of the cumulative amount of drug permeated, flux rate, permeability coefficient (Kp), and enhancement ratio (Er) were calculated, and the results are shown in Table 7. The results indicate that

Table 6 The correlation coefficient (r^2) of different kinetic models of different formulae.

MODELS	NEG-A2X	NEG-A2Y	NEG-A2Z	STANDARD SOLUTION	MARKETED SOLUTION	NE-A2
Zero order	0.7830	0.7406	0.7427	0.3926	0.4509	0.7435
First order	0.9328	0.9198	0.9201	0.8965	0.6056	0.9612
Higuchi	0.9444	0.9271	0.9214	0.6163	0.6808	0.9189
Korsmeyer	0.2490	0.2023	0.1976	0.0692	0.1020	0.2280

The comparison was made between optimized MXD-loaded NE formula (NE-A2), alcoholic standard solution, marketed solution and NEG formulations (NEG-A2x, NEG-A2y, and NEG-A2z) that released in phosphate buffer solution pH 7.4 (0.2M)

Table 7 Permeation parameters for MXD from the optimized MXD-loaded NEG formula (NEG-A2y) and marketed solution.

PERMEATION PARAMETERS	FORMULATION	
	NEG-A2y	Marketed solution
Cumulative amount (Q, µg/cm²)	961.97±4.77*	398.24±10.038
Flux rate (Jss, µg/cm²/h)	38.005±0.02*	16.54±0.45
Permeability coefficient Kp (cm²/h) *10⁻³	3.80±0.0023*	1.65±0.045
Enhancement ratio (Er)	2.3±0.06	

Data expressed as mean±SD. * P≤0.05 as compared to marketed solution

the steady state transdermal flux (SSTF) for the NEG-A2y formula was significantly higher (P≤0.05) than the marketed solution. The permeability coefficient Kp was also significantly higher for NEG-A2y in comparison to the marketed solution. Overall, the permeation enhancement ratio from the NEG-A2y formulation to the marketed solution was 2.3 ±0.06-fold.

The results of this study are consistent with those of Kaur *et al.*, who developed a transdermal NEG formulation of fluvastatin with nano-sized globules and concluded that their NEG formulation significantly improved permeation compared to a conventional solution formulation (46). Similar findings were also reported by Morsy *et al.*, in a study in which they concluded that the skin permeation potential of atorvastatin was significantly enhanced when formulated into a NEG compared to a solution (53).

Several factors were involved in designing our prototype NEG formulation for achieving an improved MXD topical delivery profile compared to the marketed product. Because permeability is inversely proportional to the size of the formulation droplets, nano-sized droplets of the optimized MXD-loaded NE formula (NE-A2) may facilitate MXD penetration through skin layers and improve the drug permeation characteristics. Nanosizing of droplets increases their surface area and therefore the amount of material in contact with the skin for drug penetration to occur, (128). The incorporation of NE into Carbopol® 934 showed further improvement in ex vivo permeation due to higher retention and contact time with skin. Other factors influencing local drug availability are related to the solubility of MXD in the various excipients in the NEG formulation and the local drug concentrations achieved. In addition, various components were included in the NEG to influence the permeability of the skin. For instance, the presence of a non-ionic surfactant (i.e. Tween® 80) in the NE formulation may improve the permeation of MXD through the skin because surfactant monomers have the ability to alter the integrity and function of biological membranes

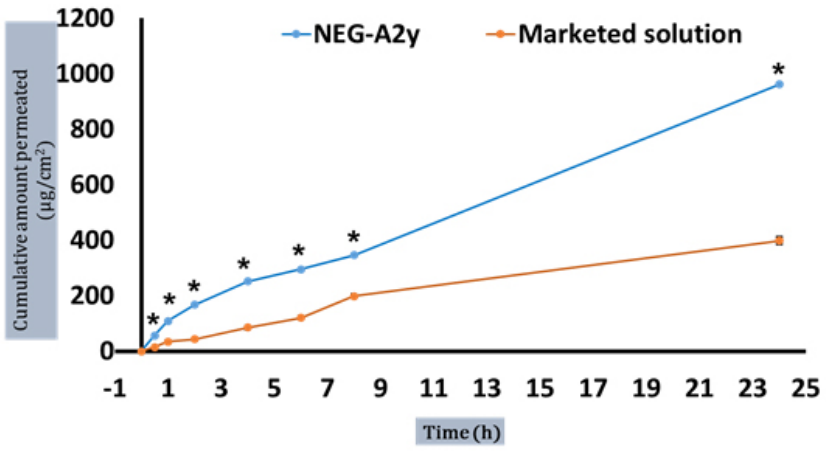

Figure 10 Permeation profiles of MXD through the excised rat skin. Both optimized NEG formula (NEG-A2y) and marketed solution were tested. Data expressed as mean±SD. * P≤0.05 as compared to marketed solution.

Table 8 Physical characterization of the optimized MXD-loaded NEG formula (NEG-A2y) following 3months of storage at 6°C, 25°C and 45°C.

PARAMETER		6±2°C	25±2°C	45±2°C
	DAY 0	DAY 30	DAY 60	DAY 90
Color	Light yellow	Light yellow	Light yellow	Light yellow
Homogeneity	Homogenous	Homogenous	Homogenous	Homogenous
pH	6±0.08^{ns}	6±0.23^{ns}	5.9±0.8^{ns}	5.9±0.52^{ns}
Electrical conductivity µS/cm	52±0.72*	54±0.39	56±0.34	53±0.53$^{\#}$

*p≤0.05 as compared to Day 60, #p≤0.05 as compared to Day 30 and 60, ns=non-significant. Data are expressed as mean ±SD

to facilitate drug transport across them(54). Similarly, permeability may be increased due to the presence of clove oil, which contains eugenol, that has the ability to permeate the skin and increase partitioning of through the SC into the deeper skin layers (55). Moreover, the presence of co-solvent PG in the formulation may improve drug partitioning into skin layers through a variety of processes including lipid and protein extraction and SC swelling (56). In summary, the improved skin permeation could be due to the various multifunctional components of the NEG such as clove oil, Tween® 80 and propylene glycol that act synergistically and manifest penetration enhancement through the SC (7).

Stressed Stability study

The MXD-loaded NEG formula (NEG-A2y) was subjected to a stressed stability study at different storage conditions and the physical characteristics of the nanoemulsion were assessed in compliance with ICH guidelines. The data from the stability testing are shown in Table 8. The formulation NEG-A2y was checked visually, and the results showed no significant change in color, homogeneity and pH at the different temperatures (i.e. 6°C, 25°C, and 45°C) in comparison to a freshly prepared formulation. Some changes in electrical conductivity measurements (p≤0.05) were observed in different storage conditions, but this difference is not relevant because values remained well above 10 µS/cm, indicating that the emulsion was maintained as an o/w composition. Based on the tests performed, the NEG showed excellent stability with no evidence of physical instability over 90 days. Incorporation of a gelling agent in NEG-A2y may have played a role in maintaining physical stability as this topic has been highlighted by Mohamed *et al.*, and their work demonstrating the critical role of gelling agents in nanoemulsion stability (57).

CONCLUSIONS

The development of a prototype topical nanoemulsion formulation of minoxidil was achieved using a formulation comprising of clove oil, Tween® 80, ethanol and propylene glycol. The formulation demonstrated appropriate physical properties (nanometer size, acceptable polydispersity, etc), good compatibility (neutral pH with precedented excipients), etc. To overcome issues typically associated with topical formulations, namely short contact time, the nanoemulsion was modified to include a gelling component, Carbopol® 934, to increase viscosity, and to aid in reducing drug losses at the site of action. Drug delivery performance of this nanoemulgel, NEG-A2y, was significantly better than that of a currently marketed product with the nanoemulgel giving a 2.3 fold enhancement of drug delivery in the ex vivo drug permeability study. This work highlights the importance of formulation design in preparing nanoemulsions for topical drug delivery. Furthermore, these studies highlight the value of incorporating a polymer excipient, such as Carbopol®, to create a nanoemulsion-based gel system to improve local drug concentrations and enhance overall drug delivery efficiency.

ACKNOWLEDGMENTS

The authors wish to thank the University of Mosul for providing the facilities to undertake this work.

REFERENCES

1 Suchonwanit P, Thammarucha S, Leerunyakul K. Minoxidil and its use in hair disorders: A review. Drug Des Devel Ther, 13:2777–86, 2019.

2 Jackson R V, Williamson MM, Seneviratne B, Gordon RD. Long term minoxidil therapy and renal function, cardiac function, hypertrichosis and blood pressure. Aust N Zeal J Med, 13(1):39–44, 1983.

3 Friedman ES, Friedman PM, Cohen DE, Washenik K. Allergic contact dermatitis to topical minoxidil solution: etiology and treatment. J Am Acad Dermatol, 46(2):309–12, 2002.

4 Sunitha S, Jitendra W, Sujatha D, Kumar MS. Design and Evaluation of Hydrogel-Thickened Microemulsion for Topical Delivery of Minoxidil. Iran J Pharm Sci, 9(4):1–14, 2013.

5 Cardoso SA, Barradas TN. Developing formulations for drug follicular targeting: Nanoemulsions loaded with minoxidil and clove oil. J Drug Deliv Technol, 59:101908, 2020.

6 de Oca-Ávalos JMM, Candal RJ, Herrera ML. Nanoemulsions: Stability and physical properties. Curr Opin Food Sci, 16:1–6, 2017.

7 Khurana S, Jain NK, Bedi PMS. Nanoemulsion based gel for transdermal delivery of meloxicam: physico-chemical, mechanistic investigation. Life sciences, 92(6–7):383–92, 2013.

8 Mou D, Chen H, Du D, Mao C, Wan J, Xu H, et al. Hydrogel-thickened nanoemulsion system for topical delivery of lipophilic drugs. Int J Pharm, 353(1–2):270–6, 2008.

9 Joshi B, Singh G, Rana AC, Saini S, Singla V. Emulgel: a comprehensive review on the recent advances in topical drug delivery. Int Res J Pharm, 2(11):66–70, 2011.

10 Eid AM, El-Enshasy HA, Aziz R, Elmarzugi NA. Preparation, characterization and anti-inflammatory activity of Swietenia macrophylla nanoemulgel. J Nanomed Nanotechnol, 5(2):1–10, 2014.

11 Mahesh B, Vasanth KP, Gowda D V, Atul S, Raghundan H V, Chetan SG. Enhanced permeability of cyclosporine from a transdermally applied nanoemulgel. Pharm Sin, 6:69–79, 2015.

12 Bashir M, Ahmad J, Asif M, Khan SUD, Irfan M, Ibrahim AY, et al. Nanoemulgel, an Innovative Carrier for Diflunisal Topical Delivery with Profound Anti-Inflammatory Effect: in vitro and in vivo Evaluation. Int J Nanomedicine, 16:1457, 2021.

13 Elmataeeshy ME, Sokar MS, Bahey-El-Din M, Shaker DS. Enhanced transdermal permeability of Terbinafine through novel nanoemulgel formulation; Development, in vitro and in vivo characterization. Future J Pharm Sci, 4(1):18–28, 2018.

14 Adak T, Barik N, Patil NB, Gadratagi BG, Annamalai M, Mukherjee AK, et al. Nanoemulsion of eucalyptus oil: An alternative to synthetic pesticides against two major storage insects (Sitophilus oryzae (L.) and Tribolium castaneum (Herbst)) of rice. Ind Crops Prod, 143:111849, 2020.

15 Paliwal S, Kaur G, Arya RK. K, Formulation and characterization of topical nanoemulgel of terbinafine. Univers J Pharm Res, 3(6):28–37, 2018.

16 Branco IG, Sen K, Rinaldi C. Effect of sodium alginate and different types of oil on the physical properties of ultrasound-assisted nanoemulsions. Chem Eng Process, 153:107942, 2020.

17 Sarheed O, Dibi M, Ramesh KV. Studies on the Effect of Oil and Surfactant on the Formation of Alginate-Based O/W Lidocaine Nanocarriers Using Nanoemulsion Template. Pharmaceutics, 12(12):1223, 2020.

18 Séguy L, Groo AC, Goux D, Hennequin D, Malzert-Fréon A. Design of Non-Haemolytic Nanoemulsions for Intravenous Administration of Hydrophobic APIs. Pharmaceutics, 12(12):1141, 2020.

19 Khatoon K, Ali A, Ahmad FJ, Hafeez Z, Rizvi MMA, Akhter S, et al. Novel nanoemulsion gel containing triple natural bio-actives combination of curcumin, thymoquinone, and resveratrol improves psoriasis therapy: in vitro and in vivo studies. Drug Deliv and Transl Res, 11(3):1245–60, 2021.

20 Karami Z, Saghatchi Zanjani MR, Nasihatsheno N, Hamidi M. Improved oral bioavailability of repaglinide, a typical BCS Class II drug, with a chitosan coated nanoemulsion. J Biomed Mater Res B Appl Biomater, 108(3):717–28, 2020.

21 Dadwal A, Mishra N, Rawal RK, Narang RK. Development and characterisation of clobetasol propionate loaded Squarticles as a lipid nanocarrier for treatment of plaque psoriasis. J Microencapsul, 37(5):341-54, 2020.

22 Algahtani MS, Ahmad MZ, Ahmad J. Nanoemulgel for improved topical delivery of retinyl palmitate: formulation design and stability evaluation. Nanomaterials, 10(5):848, 2020.

23 Al-Nima AM, Al-Kotaji M, Al-Iraqi O, Ali ZH. Preparation and evaluation of ultrasound transmission gel. Asian J Pharm Clin Res, 12(1):422–7, 2019.

24 Soliman WE, Shehata TM, Mohamed ME, Younis NS, Elsewedy HS. Enhancement of Curcumin Anti-Inflammatory Effect via Formulation into Myrrh Oil-Based Nanoemulgel. Polymers, 13(4):577, 2021.

25 Manyarara TE, Khoza S, Dube A, Maponga CC. Formulation and characterization of a paediatric nanoemulsion dosage form with modified oral drug delivery system for improved dissolution rate of nevirapine. MRS Advances, 3(37):2203–19, 2018.

26 Gouda R, Baishya H, Qing Z. Application of mathematical models in drug release kinetics of carbidopa and levodopa ER tablets. J Dev Drugs, 6(02):1–8, 2017.

27 Soni K, Mujtaba A, Akhter MH, Zafar A, Kohli K. Optimisation of ethosomal nanogel for topical nano-CUR and sulphoraphane delivery in effective skin cancer therapy. J Microencapsul, 37(2):91–108, 2020.

28 Rambharose S, Kalhapure RS, Govender T. Nanoemulgel using a bicephalous heterolipid as a novel approach to enhance transdermal permeation of tenofovir. Colloids Surf B: Biointerfaces, 154:221–7, 2017.

29 Mulleria SS, Marina K, Ghetia SM. Formulation, Optimization and in vitro Evaluation of Apremilast Nanoemulgel for Topical Delivery. Int J Pharm Investig, 2021;11(2):230–7, 2021.

30 Shahtalebi MA, Sadat-Hosseini A, Safaeian L. Preparation and evaluation of clove oil in emu oil self-emulsion for hair conditioning and hair loss prevention. J Herbmed Pharmacol, 5(2):72–7, 2016.

31 Nagaraju PG, Sengupta P, Chicgovinda PP, Rao PJ. Nanoencapsulation of clove oil and study of physicochemical properties, cytotoxic, hemolytic, and antioxidant activities. J Food Process Eng, 44(4):e13645, 2021.

32 Zdrali E, Etienne G, Smolentsev N, Amstad E, Roke S. The interfacial structure of nano-and micron-sized oil and water droplets stabilized with SDS and Span80. J Chem Phys, 150(20):204704, 2019.

33 Khames A. Formulation and characterization of eplerenone nanoemulsion liquisolids, an oral delivery system with higher release rate and improved bioavailability. Pharmaceutics. 11(1):40, 2019.

34 Jaipakdee N, Limpongsa E, Pongjanyakul T. Optimization of minoxidil microemulsions using fractional factorial design approach. Pharm Dev Technol, 21(1):86–97, 2016.

35 Hassan AK. Effective surfactants blend concentration determination for o/w emulsion stabilization by two nonionic surfactants by simple linear regression. Indian J Pharm Sci, 77(4):461, 2015.

36 Li C, Wang Y, Sha S, Yin H, Zhang H, Wang Y, et al. Analysis of the tendency for the electronic conductivity to change during alcoholic fermentation. Sci Rep, 9(1):1–8, 2019.

37 Patel RJ, Parikh RH. Intranasal delivery of topiramate nanoemulsion: Pharmacodynamic, pharmacokinetic and brain uptake studies. Int J Pharm, 585:119486, 2020.

38 Sadoon NA, Ghareeb MM. Formulation and Characterization of Isradipine as Oral Nanoemulsion. Iraqi J Pharm Sci, 29(1), 2020.

39 Hasani F, Pezeshki A, Hamishehkar H. Effect of surfactant and oil type on size droplets of betacarotene-bearing nanoemulsions. Int J Curr Microbiol App Sci, 4(9):146–55, 2015.

40 Yuan Y, Li S ming, Mo F kui, Zhong D fang. Investigation of microemulsion system for transdermal delivery of meloxicam. Int J Pharm, 321(1–2):117–23, 2006.

41 Avachat AM, Patel VG. Self nanoemulsifying drug delivery system of stabilized ellagic acid–phospholipid complex with improved dissolution and permeability. Saudi Pharm J, 23(3):276–89, 2015.

42 Najafi Z, Kahn CJF, Bildik F, Arab-Tehrany E, Şahin-Yeşilçubuk N. Pullulan films loading saffron extract encapsulated in nanoliposomes; preparation and characterization. Int J Biol Macromol, 188:62–71, 2021.

43 Tabilo-Munizaga G, Villalobos-Carvajal R, Herrera-Lavados C, Moreno-Osorio L, Jarpa-Parra M, Pérez-Won M. Physicochemical properties of high-pressure treated lentil protein-based nanoemulsions. LWT. 101:590–8, 2019.

44 Parmar N, Singla N, Amin S, Kohli K. Study of cosurfactant effect on nanoemulsifying area and development of lercanidipine loaded (SNEDDS) self nanoemulsifying drug delivery system. Colloids Surf B: Biointerfaces, 86(2):327–38, 2011.

45 Md S, Alhakamy NA, Aldawsari HM, Kotta S, Ahmad J, Akhter S, et al. Improved analgesic and anti-inflammatory effect of diclofenac sodium by topical nanoemulgel: Formulation development—In vitro and in vivo studies. J Chem, 2020:1-10, 2020.

46 Kaur R, Ajitha M. Transdermal delivery of fluvastatin loaded nanoemulsion gel: Preparation, characterization and in vivo anti-osteoporosis activity. Eur J Pharm Sci, 136:104956, 2019.

47 Jacobs C, Kayser O, Müller RH. Nanosuspensions as a new approach for the formulation for the poorly soluble drug tarazepide. Int J Pharm, 196(2):161–4, 2000.

48 Wik J, Bansal KK, Assmuth T, Rosling A, Rosenholm JM. Facile methodology of nanoemulsion preparation using oily polymer for the delivery of poorly soluble drugs. Drug Deliv Transl Res, 10(5):1228–40, 2020.

49 Md S, Alhakamy NA, Aldawsari HM, Husain M, Kotta S, Abdullah ST, et al. Formulation design, statistical optimization, and in vitro evaluation of a naringenin nanoemulsion to enhance apoptotic activity in A549 lung cancer cells. Pharmaceuticals, 13(7):152, 2020.

50 Kumar M, Bishnoi RS, Shukla AK, Jain CP. Development and optimization of drug-loaded nanoemulsion system by phase inversion temperature (PIT) method using Box–Behnken design. Drug Dev Ind Pharm, 47(6):977–89, 2021.

51 Bhattacharya S, Prajapati BG. Formulation and optimization of celecoxib nanoemulgel. Asian J Pharm Clin Res, 10(8):355–6, 2017.

52 Küchler S, Herrmann W, Panek-Minkin G, Blaschke T, Zoschke C, Kramer KD, et al. SLN for topical application in skin diseases—Characterization of drug–carrier and carrier–target interactions. Int J Pharm, 390(2):225–33, 2010.

53 Morsy MA, Abdel-Latif RG, Nair AB, Venugopala KN, Ahmed AF, Elsewedy HS, et al. Preparation and evaluation of atorvastatin-loaded nanoemulgel on wound-healing efficacy.

Pharmaceutics, 11(11):609, 2019.

54 Balakrishnan P, Shanmugam S, Lee WS, Lee WM, Kim JO, Oh DH, et al. Formulation and in vitro assessment of minoxidil niosomes for enhanced skin delivery. Int J Pharm, 377(1–2):1–8, 2009.

55 Meer S, Akhtar N. Annona muricata extract containing pharmaceutical emulgels with and without penetration enhancer for depigmenting and antierythmic effects. Pak J Pharm Sci, 2018.

56 Kováčik A, Kopečná M, Vávrová K. Permeation enhancers in transdermal drug delivery: Benefits and limitations. Expert Opin Drug Deliv, 17(2):145–55, 2020.

57 Mohamed MI. Optimization of chlorphenesin emulgel formulation. The AAPS journal, 6(3):81–7, 2004.